Generation of conical second harmonic waves by nonlinear Bragg diffraction in two-dimensional nonlinear photonic structures

Solomon M. Saltiel [a,b], Dragomir N. Neshev [a], Wieslaw Krolikowski [a], Robert Fischer [a], Ady Arie [c], and Yuri S. Kivshar[a]

[a]Nonlinear Physics Center and Laser Physics Centre, Centre for Ultra-high bandwidth Devices for Optical Systems (CUDOS), Research School of Physical Sciences and Engineering, Australian National University, Canberra ACT 0200, Australia;
[b]Department. of Quantum Electronics, Faculty of Physics, Sofia University, Bulgaria
[c]School of Electrical Engineering, Faculty of Engineering, Tel-Aviv University, Ramat Aviv, Tel-Aviv, Israel

ABSTRACT

We generate conical second-harmonic waves through the parametric frequency conversion in a two-dimensional annular, periodically poled nonlinear photonic structure under the transverse excitation with a fundamental Gaussian beam. We explain the effects observed experimentally by applying the concept of nonlinear Bragg diffraction to the case of the conical frequency generation. We study the polarization properties of the conical emission at the second-harmonic frequency and demonstrate that each of the parametrically generated waves represents a superposition of the Bessel beams.

Keywords: Nonlinear optics, Second harmonic generation, Bessel beams.

1. INTRODUCTION

The effect of the Bragg diffraction is usually observed for the propagation of linear waves in media with a periodic change of the optical refractive index [1]. For certain incidence angles, the partial refracted waves add coherently and form a strong beam propagating outside the sample at the angles $\beta_m=\sin^{-1}(m\lambda/\Lambda)$ where λ is the wavelength, Λ is the modulation period, and *m* is an integer number. Importantly, the similar Bragg diffraction can also occur in media with a spatially homogeneous optical refractive index which have nonlinear properties varying periodically. This effect, known as *nonlinear Bragg diffraction* was first discussed by Freund [2], and it was observed experimentally in naturally laminated crystals exhibiting non-regularity and dispersion of the nonlinear domains [2-4]. Recently, nonlinear diffraction has also been reported in second- and third-harmonic generation in the presence of transient optically-induced one-dimensional grating [5]. Nonlinear diffraction is observed also in photonic crystals with simultaneous modulation of both linear and nonlinear properties [4-7]

Here we study theoretically and observe experimentally the nonlinear Bragg diffraction for the conical second-harmonic generation (SHG) in a two-dimensional nonlinear photonic structure [8,10,11] fabricated in a periodically poled stoichiometric Lithium Tantalate (SLT) crystal with the annular periodic modulation of the second-order nonlinear response. We observe that a transverse illumination of a radially periodic structure [see the image (a) in Fig.1 by a strong Gaussian beam leads to *multiple conical emission* of the second-harmonic (SH) waves [see the photo (b) in Fig.1. These SH waves form a set of rings in the far-field zone, and the angles of their propagation satisfy the well-known Bragg relation, i.e they are determined by a ratio of the second-harmonic wavelength to the period of the nonlinearity modulation. We study the polarization properties of the diffracted SH rings and demonstrate that they are defined, in a complex way, by the input polarization and the second-order nonlinear susceptibility tensor. In a general case, the polarization varies with the azimuthal angle of the ring. Moreover, we show theoretically that in such an annular quasi-phase-matched structure the field inside the sample consists of the Bessel beams of different widths, so that the observed diffraction rings are the far-field images of the second-harmonic Bessel beams generated inside the nonlinear crystal.

Photonics: Design, Technology, and Packaging III
edited by Wieslaw Z. Krolikowski, Costas M. Soukoulis, Ping Koy Lam, Timothy J. Davis, Shanhui Fan, Yuri S. Kivshar
Proc. of SPIE Vol. 6801, 680113, (2008) · 0277-786X/08/$18 · doi: 10.1117/12.759281

2. EXPERIMENT

We consider a planar photonic structure with a two-dimensional periodic modulation of the second-order nonlinearity but homogeneous linear refractive index. In general, two-dimensional quasi-phase-matched (QPM) photonic structures have been suggested and explored exclusively for the *longitudinal* geometry when the input beam is directed perpendicular to the domains of periodically varying second-order nonlinearity. Here, we explore a novel *transverse* geometry for the two-dimensional nonlinear photonic crystal formed by a circularly periodic poled structure.

To explain the observed SH diffraction rings observed in experiment described below, we consider the phase-matching (PM) conditions for the corresponding SHG process. The sample with annular QPM structure [9] with the period Λ is excited with an intense laser beam. In contrast to Ref.[9], the beam is directed along the axial symmetry axis of the structure [12] that is also axis *Z* of the crystal. The general vectorial phase-matching condition $2\mathbf{k}_1+\mathbf{G}_m + \Delta\mathbf{k}_m = \mathbf{k}_2^{(m)}$ with $\mathbf{k}_1$ and $\mathbf{k}_2^{(m)}$ wave-vectors of the fundamental and SH waves, $\mathbf{G}_m$ the m-order of reciprocal vector of the $\chi(2)$ modulation $\mathbf{G}_m = m(2\pi/\Lambda)$, $\Delta\mathbf{k}_m$ the mismatch and *m* the order of the generated SH wave. This phase matching condition will be analyzed by splitting it into the transverse: $k_2\sin\alpha_m = G_m = mG_1$, and the longitudinal: $k_2\cos\alpha_m - 2\mathbf{k}_1 = \Delta k_m$ phase-matching conditions [13]. With a correct choice of the fundamental wavelength or crystal temperature, a given diffraction order will be longitudinally phase-matched with $\Delta k_m = 0$. As an example, in Fig.1(c), the third diffraction order SH process is phase-matched ($\Delta k_3 = 0$) and for this interaction both PM conditions are satisfied simultaneously. Inside the crystal, the propagation angles of all transversely phase-matched waves are found from the relation, $\sin\alpha_m = m\lambda_2 / n_2\Lambda$. Outer angles are: $\beta_m = \sin^{-1}(m\lambda_2/\Lambda)$ that coincide with the formula for the Bragg diffraction. The maximum numbers of the SH rings exiting from the flat output surface is $M_1 = \Lambda/\lambda_2$. The SHG process in the transverse direction determines the total maximum diffraction orders, $M_2 = n_2\Lambda/\lambda_2$. For this transverse SHG the longitudinal fundamental mismatch will be $\Delta k_m = 2\mathbf{k}_1$. Its compensation is possible when two counter-propagating fundamental waves are used [14-17].

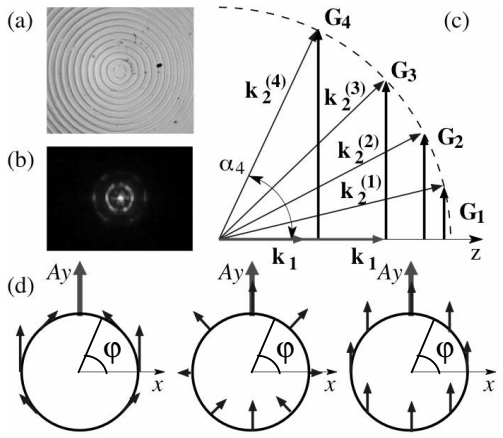

Fig. 1. (a) Front facet of the SLT sample. (b) A photo of the first two diffraction SH rings. (c) Phase-matching diagram of the SHG process in the transverse QPM grating. (d) Polarization structure of the ``ordinary'' (left), ``extraordinary'' (middle), and small-angle (right) SH rings. Fundamental wave (red) has the Y polarization.

The discussion so far considered the phase-matching conditions in single plane (single azimuthal angle φ defined in Fig. 1). Since the structure is annularly periodically poled and it is suggested that excitation is in the centre of the structure the conclusions will be valid for any azimuthal angle φ and consequently the SH radiation will appear in form of concentric cones with cone angles β_m.

In Fig. 2(a) it is shown photo of the first two orders SH conical waves and the 13-th order SH conical wave that is both longitudinally and transversely phase-matched. The fundamental beam is exactly in the center of the structure. The photo

on Fig. 2(b) is taken when the beam is shifted from the center. In this case the process of SHG should be considered as result of interaction of the fundamental beam with one dimensional periodical poled grating. As a result instead of rings we record line of diffracted spots. More than 7 consecutive orders are seen. The two strong points at both sides of the photo correspond to the 13-th order nonlinear SH diffraction. Below the photo it is shown the microdensitogram demonstrating the relative intensities of the diffracted spots. These intensities should be compared with the theoretical predictions shown on Fig. 2(c), where the dependencies of the wave vector mismatch and the predicted SH efficiency normalized to the first-order SH signal (in log scale) as a function of the diffraction order are shown.

The outer rings possess interesting polarization properties defined by the tensor of the second-order nonlinearity of the Lithium Tantalate crystal. This crystal belongs to the 3m symmetry point group. For the fundamental beam propagating along the axis Z, it has the following relevant nonzero components: $d_{xxz} = d_{yyz}$, $d_{xxy} = d_{yxx} = -d_{yyy}$. Note that in periodical poled crystals with 3m symmetry d_{xxy}, d_{yxx}, d_{yyy} also change sign [18]. Two types of the SH processes are possible: Type I [(oo-e), two ordinary waves generate an extraordinary SH wave] and Type 0 [(oo-o), two ordinary waves generate an ordinary SH wave)]. Effective nonlinearities can be found following the method described in [19]

$$d_{eff}^{(o)} = d_{yyy}\cos(\varphi + 2\gamma) \tag{1}$$

$$d_{eff}^{(e)} = d_{yyy}\cos\alpha\sin(\varphi + 2\gamma) + d_{zyy}\sin\alpha \tag{2}$$

where φ is the azimuthal angle counted from the X axis, α is the diffracted angle inside the crystal, and γ is the angle that defines the orientation of the input beam polarization plane (for the fundamental wave polarized along X, γ=0).

The azimuthal intensity distribution of the ordinary and extraordinary SH depends on the input polarization defined by the angle γ. Since the two rings are orthogonally polarized the total intensity is given as

$$I_{2\omega,m}^{(o)} \propto \left(S^{(e)}\left[d_{eff}^{(e)}\right]^2 + S^{(o)}\left[d_{eff}^{(o)}\right]^2 \right) I_1^2 g_m^2 L^2 \quad , \tag{3}$$

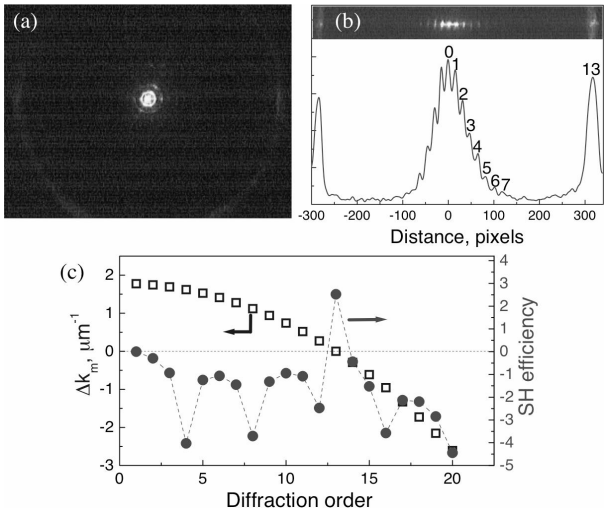

Fig. 2. Experimentally observed SH rings. The axis X is horizontal. (a) Fundamental beam is exactly in the center of the annular structure: first several orders and 13-th order SH ring are seen; (b) the sample is shifted horizontally. The diffraction patterns corresponding to first 7 orders and the 13-th order nonlinear Bragg diffraction. (c) Dependencies of the wave vector mismatch and the predicted SH efficiency normalized to the first-order SH signal (in log scale) as a function of the diffraction order. The 13-th order SHG process by nonlinear Bragg diffraction is phase-matched both longitudinally and transversely.

where $S^{(o,e)} = \sin^2(2\pi L / L_{coh}^{(o,e)}) / \left(\pi L / L_{coh}^{(o,e)}\right)^2$, $L_{coh}^{(o,e)} = \pi / \Delta k_m^{(o,e)}$, and $g_m = 2/(\pi m)\sin(\pi m D)$ with D being the duty factor. In Fig.2(c) we illustrate the dependence of the relative intensity $I_{2\omega,m}^{(o)}$ (in log scale) in each diffraction order m assuming for simplicity that the length of the sample is a multiple of the coherence length L_{coh}.

For small angles α, when we can neglect a difference in the refractive indices of the two waves, the polarization of the whole ring will be linear. For γ = 0 and γ = π/2 polarization at any φ will be directed along Y, and for γ = π/4 along X-directions. The intensity of the total ring does not depend on the orientation of the input polarization. For relatively large α each of the rings propagates with its own phase velocity [$n_o > n_e(\alpha)$] and at slightly different internal angles. In this case, the output polarization as a function of the azimuthal angle depends also on the actual overlap of the two rings at the output surface since the ordinary and extraordinary rings will be tangentially and radially polarized, respectively. In Fig.1(d) we show the structure of the predicted polarization ring for the ratio $d_{yyy}/d_{zyy} \cong -1.7$ [20] and large enough angle α not to allow neglecting the second term of Eq.(2). For relatively long crystals every diffraction order should appear as a doublet of two cross-polarized rings.

The wave vectors of SH waves emitted by the annular PPLT lay on a cone with a conical angle α. It is known that a superposition of an infinite number of plane waves with the wave vectors laying on a cone results in a formation of a Bessel beam [21,22]. A more detailed analysis of the SHG process in the structure with the azimuthal symmetry shows that, as a matter of fact, the SH wave inside the crystal has a form of a Bessel beam [12]. In the case discussed earlier for the Strontium Barium Niobate (SBN) crystal, the crystal symmetry caused the SH wave to be represented by just the first-order Bessel function with a perfect radial polarization [12]. In the case of LiTaO3 or LiNbO3, the beam structure is more complicated due to the superposition of several components of the χ(2) tensor. However, it still can be represented in terms of a superposition of the low-order Bessel functions with the angularly modulated intensity. The exact formulas are quite cumbersome, but they can be simplified in the case of small emission angles when $\tan\alpha_m << 1$,

$$E(\rho,\theta_0,z) = 2\pi A^2 d_{yyy} J_0(\xi)\left[\vec{u}_x \sin 2\gamma + \vec{u}_y \cos 2\gamma\right], \tag{4}$$

where $\xi = k_2 \rho \sin\alpha$ and $\rho = (x^2+y^2)^{1/2}$ is the transverse radial coordinate. It is clear that the beam represented by Eq.(4) is linearly polarized, and its intensity is independent of the azimuthal coordinate

$$I_{2\omega} = 4 d_{yyy}^2 \pi^2 A^4 J_0^2(\xi), \tag{5}$$

what agrees completely with experimental observations.

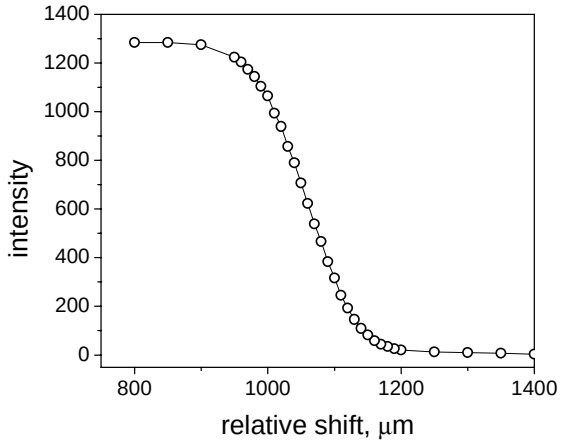

Fig. 3. Illustration of the measurement of the beam size diameter with the knife-edge method.

The Stoichiometric Lithium Tantalate (SLT) sample is described in [9]. It is thick L = 0.49 mm, with a QPM period of 7.5 μm. Duty factor varies inside the sample from 0.7 at Z+ surface to 0.8 at Z- surface. Z+ and Z- surfaces are polished. Small 20 nm deep grooves remained after polishing that cause slight fundamental diffraction at angle twice the 1 order SH diffraction. Intensity of the diffracted wave is less 3%.

To observed these effects, we employ an experimental setup that consists of Mira Ti:Sapphire laser with regenerative amplifier. It delivers femtosecond pulses with duration of 140 fs and frequency 250 kHz. The time bandwidth product is 0.49. Average output power is 740 mW. The radiation was focused in the sample with 30 cm lens. The beam waist size at the place of the sample measured with the knife-edge method is 147 μm (FWHM) as illustrated in Fig. 3. The measured beam diameter corresponds to about 100 GW/cm^2 of intensity. This figure also illustrates the good quality Gaussian shape of the fundamental beam.

The observed SH rings with laser tuned at 822 nm are shown in Fig.2(a). The cone angle is measured by recording a ring diameter as a function of the distance from the sample. In this way we define that the largest ring is phase matched for the 13-th order. Its cone angle is measured to be 45.6° (and it is slightly different from the predicted angle of 45.4° by simple re-scaling the lower-order diffraction patterns. In the same time calculated (with the use of the data for the refractive index of SLT [23]) phase matching for the 13-th order SH wave gives the phase-matching wavelength 836 nm with the cone angle 46.4°. We attribute this difference for the wavelength and angle with the absence of good Sellmeier equations for the ordinary index of refraction. The calculated longitudinal mismatch and relative intensity of the diffracted rings are shown in Fig.2(c) for λ = 836 nm. It is seen the 13-th order SH ring is phase-matched with $\Delta k_{13} = 0$, and it has the maximum intensity.

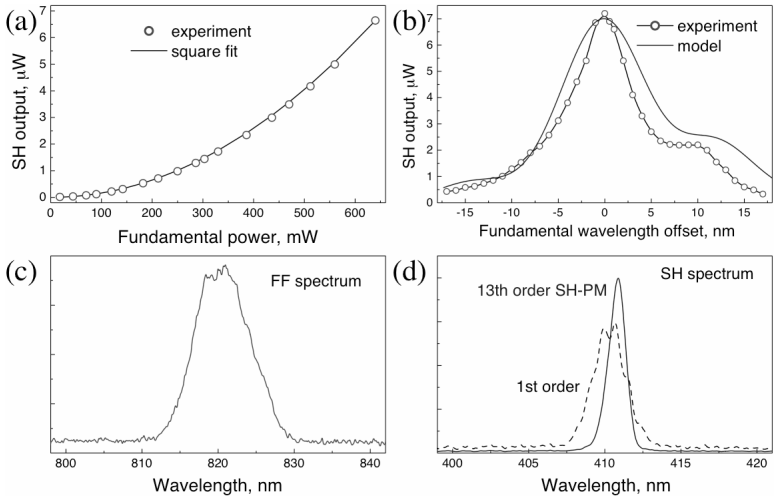

Fig. 4. (a)Quadratic dependence of the 13-th order SH ring. (b) Experimental phase matching curve and theoretical prediction normalized to the maximal point of the experiment. (c) Spectrum of the fundamental radiation. (d) Spectra of the SH rings for non phase matched (first-order) and phase matched (13-th order) SH rings.

The phase-matching curve is shown in Fig. 4(b) together with the theoretical prediction based on the model from Ref.[12] for zero offset in the production of the grating and for the duty factor 0.748. We observe strong similarity of the experimental curve and the prediction for zero offset. The difference in the phase matching wavelength (822.2 nm - experimental and 836 nm -theoretical), as we already discussed, is most likely due to uncertainty in the value of the ordinary refractive index caused by the lack of accurate corresponding Sellmeier equations. In Fig. 4(a) we verify a quadratic dependence of the SH power of the phase matched 13-th SH ring as a function of the input power. From this figure (obtained at 640 mW fundamental power taking into account of all losses), we obtain the internal efficiency for

the phase-matched 13-th order SH ring, η_{13} = 0.0036%. Such low efficiency is attributed to the fact that we use 13-th order QPM interaction and the duty factor varies inside the crystal that leads to the effective length 2-3 times less than the real sample thickness. The measured efficiency of the SH power generated in the first-order ring is 220 times less than η_{13}. Our estimation shows that for a 1 mm-long sample operating in the regime of the first order QPM with homogeneous 50% duty factor a 10% efficiency of the SH generation could be achieved.

The spectra are shown in Fig. 4(c,d). The fundamental spectral width is 8 nm. The spectra of the SH ring in the case of phase-matching of the 13-th order is 1.3 nm; i.e. almost 2 times less than it should be expected for a stationary process. This means that the SHG process takes place in the group-velocity mismatch conditions. Indeed, calculated group-velocity-mismatch length is 0.092 mm for 140 fs fundamental pulse width, that is a half of the expected effective length of the sample and the expected reduction of the spectra (lengthening of the pulse) is also correspondingly 0.5 (2 times). In contrast to the phase-matched 13-th order ring, the spectra of non-phase matched (1-st and 2-nd order) rings do not show reduction and are close to the prediction for the stationary process, $\Delta\omega_{rm,SH}= \sqrt{2}\Delta\omega_{rm,FF}$. The reason for that is the short length of interaction equal to the coherence length, that is of the order of few micrometers.

The rings are sensitive to an axial alignment of the fundamental beam. With off-center alignment the SH efficiency is higher and the number of the observed diffracted orders increases [see Fig. 5 (b)]. For a horizontal shift of the sample, the observed diffraction spots appear horizontally. For a vertical shift of the sample, the observed diffraction spots appear vertically. This is explained by the fact that the structure resembles a one-dimensional grating formed from the sectors situated close to the horizontal (vertical) diameter of the rings. The modifications of the diffraction pattern for the phase-matched 13-th order ring are shown in Figs .5(a-c). In Figs. 5 (d,e) the experimental intensity distribution of the first- and 13-th order SH rings are shown. The theoretical prediction for the 13-th order SH ring is given by Eq. (3) and shown in Fig. 5(f). As seen the averaged trend of the azimuthal intensity distribution on Fig. 5(e) is in good accordance with the theoretical prediction shown on figure Fig.5(f) confirming the correctness of the model. The six peaks seen in Fig. 5(e) will be discussed below.

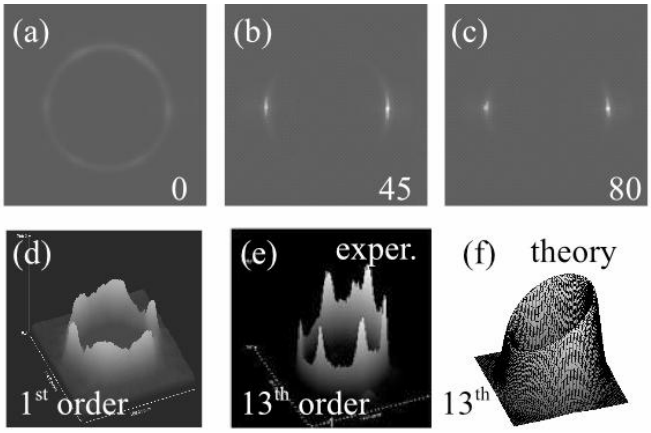

Fig. 5. (a-c) Modification of the diffraction pattern as a function of the horizontal shift. Numbers indicate the shift in μm. The sample is with horizontal *X* axis. (d,e) Experimental intensity distribution of *m=1* and *m=13* SH rings. (f) Theoretical prediction for the azimuthal intensity distribution of the *m=13* SH ring based on Eq.(3).

Another important parameter is the polarization state of the generated SH rings (see Fig. 6). As expected, for the first-order SH ring the polarization is linear when the input fundamental wave is linearly polarized. This agrees well with the formulas Eqs. (1-2) and Eq. (4) in the limit of $\alpha \to 0$. When input beam is polarized along X or Y the SH conical wave is polarized along Y. If the input fundamental beam is polarized at 45 degrees with respect to these axes the output SH conical wave is polarized along X. Polarization state becomes more complex for higher-order nonlinear diffraction as the output signal contains both ordinary and extraordinary contributions.

As can be seen from the Figs 1(b), 2(a), and 5(a,d,e) the SH rings exhibit an additional azimuthal modulation with six well-defined peaks. These peaks are insensitive to the input polarization and intensity, and they are observed even in the regime of linear diffraction of the fundamental beam on the surface relief induced by the poling pattern. Therefore they are most likely induced by the discrete character of domains boundaries resulting from the well-known ability of ferroelectric domains in the SLT [9,24] to retain their hexagonal shape.

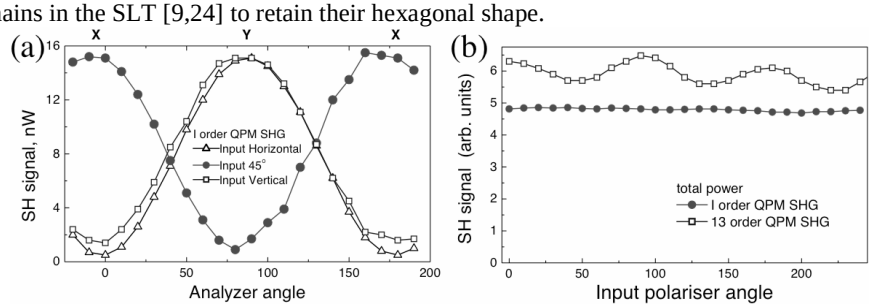

Fig. 6. Polarization properties of the SH rings: (a) Power of the 1-st order SH ring vs. analyzer angle, (b) Total power of the 1-st and 13-th order SH rings vs. the input polarization angle.

3. CONCLUSIONS

In conclusion, we have reported on the first observation of the conical second-harmonic waves generated in two-dimensional annular nonlinear photonic structures. We have explained the observed effects by employing the concept of nonlinear Bragg diffraction combined with the longitudinal and transverse phase matching conditions, and demonstrated that each of the generated waves represents a superposition of the Bessel beams. We have studied the polarization properties of the conical second-harmonic emission and demonstrated that they depend on the crystal symmetry and the cone angle. The geometry studied here may enable to generate conical harmonics in other systems including, for instance, acoustic waves in dielectrics and matter waves in optical lattices.

The work has been supported by the Australian Research Council and the Israeli Science Foundation, grant no. 960/05. We would like to thank the assistance of D. Kasimov, A. Bruner. P. Shaier and D. Eger in producing the SLT sample. S.Saltiel thanks Nonlinear Physics Center for the warm hospitality and support.

REFERENCES

1 S.A. Akhmanov and S.Yu. Nikitin, *Physical Optics* (Clarendon Press, Oxford, 1997), Chap. 16.
2 I. Freund, Phys. Rev. Lett. **21**, 1404 (1968).
3 G. Dolino, Phys. Rev. B **6**, 4025-4035 (1972).
4 Y. Le Grand, D. Rouede, C. Odin, R. Aubry, and S. Mattauch, Opt. Commun. **200**, 249-260 (2001).
5 T. Schneider and J. Reif, Phys. Rev A **65**, 023801 (2002).
6 C. Comaschi, G. Vecchi, A. M. Malvezzi, M. Patrini , G. Guizzetti, M. Liscidini, L. C. Andreani, D. Peyrade, Y. Chen, Appl. Phys. B **81**, 305 (2005).
7 A. M. Malvezzi, F. Cattaneo, G. Vecchi, M. Falasconi, G. Guizzetti, L. C. Andreani, F. Romanato, L. Businaro, E. D. Fabrizio, A. Passaseo, and M. D. Vittorio, J. Opt. Soc. Am. B **19**, 2122 (2002).
8 V. Berger, Phys. Rev. Lett. **81**, 4136 (1998).
9 D. Kasimov, A. Arie, E. Winebrand, G. Rosenman, A. Bruner, P.Shaier, and D. Eger, Opt. Express **14**, 9371 (2006).
10 N. G. R. Broderick, G. W. Ross, H. L. Offerhaus, D. J. Richardson and D. C. Hanna, Phys. Rev. Lett. **84**, 4345 (2000).
11 P. Xu, S. H. Ji, S. N. Zhu, X. Q. Yu, J. Sun, H. T. Wang, J. L. He, Y.Y. Zhu, and N. B. Ming, Phys. Rev. Lett. **93**, 133904 (2004).

[12] S. Saltiel, W. Krolikowski, D. Neshev, and Yu.S. Kivshar, Opt. Express **15**, 4132 (2007).
[13] S. P. Tewari, H. Huang, and R. W. Boyd, Phys. Rev. A **54**, 2314 (1996).
[14] R. Normandin, R. L. Williams, and F. Chatenoud, Electr. Lett. **26**, 2088 (1990).
[15] N. D. Whitbread, J. A. R. Williams, J. S. Roberts, I. Bennion, and P. N. Robson, Opt. Lett. **19**, 2089 (1994).
[16] A. Otomo, G. I. Stegeman, M. C. Flipse, M. B. J. Diemeer, W. H. G. Horsthuis, and G. R. Mohlmann, J. Opt. Soc. Am. B **15**, 7759 (1998).
[17] R. Fischer, D. N. Neshev, S. M. Saltiel, A. A. Sukhorukov, W. Krolikowski, and Yu. S. Kivshar, Appl. Phys. Lett. **91**, 031104 (2007).
[18] A. Ganany, A. Arie, S. M. Saltiel, Appl. Phys. B **85**, 97 (2006).
[19] F. Zernike, J. Midwinter, ``Applied Nonlinear Optics," John Wiley & Sons 1973.
[20] F. Charra, G. G. Gurzadyan: *Nonlinear Dielectric Susceptibilities*, Landolt-Bornstein, New Series III/30, ed. by D. F. Nelson (Springer, Berlin, Heidelberg 2000).
[21] J. Durnin, J. Opt. Soc. Am. A **4**, 651 (1987).
[22] Z. Bouchal and M. Olivik, J. Mod. Optics **42**, 1555-1556 (1995).
[23] M. Nakamura, Sh. Higuchi1, Sh. Takekawa, K. Terabe, Ya. Furukawa and K. Kitamura, Jpn. J. Appl. Phys. **41**, L465 (2002).
[24] V. Shur, E. Shishkin, I. Baturin, A. Chernykh, D. Kuznetsov, A. Lobov, A. Shur, M. Dolbilov, K. Gallo, http://eprints.soton.ac.uk/42411/